

Traffic flow stability in stochastic second-order macroscopic continuum model

MAROUANE BOUADI^a, BIN JIA^{*a}, RUI JIANG^{*a}, XINGANG LI^a, and ZI-YOU GAO^a

^aKey Laboratory of Transport Industry of Big Data Application Technologies for Comprehensive Transport, Ministry of Transport, Beijing Jiaotong University, Beijing 100044, China

Abstract

Second-order macroscopic continuum models have been constantly improved for a more realistic traffic flow modeling. Recently, a series of experimental studies have suggested that the presence of stochastic factors contributes significantly to the emergence of traffic instabilities. Nevertheless, the traffic flow stability of stochastic second-order macroscopic continuum model hasn't received the attention it deserves in past studies. More importantly, we have found that the destabilizing aspect of stochasticity is still not correctly validated in the existing theoretical stability analysis. In this paper, we analytically study the impact of stochasticity on traffic flow stability for a general stochastic second-order macroscopic model by using the direct Lyapunov method. Numerical simulations have been carried out for a stochastic speed gradient model. Our analytical stability analysis has been validated and the empirically observed concave growth pattern of traffic oscillations has been reproduced. Our methodology has been proved efficient and theoretically revealed that the presence of stochasticity indeed destabilizes the traffic flow system which is in agreement with the last empirical findings. Finally, a parsimonious stochastic speed gradient model has been calibrated and validated against empirical data. It is found that the stochastic second-order macroscopic model can successfully reproduce the empirically observed spontaneous emergence of traffic oscillations.

Keywords: Stochastic factors, Second-order macroscopic models, Stability analysis, Direct Lyapunov method.

1 Introduction

In vehicular traffic science and engineering, scholars have developed many theories to explain the complex traffic flow dynamics. Many fascinating non-linear traffic phenomena have been reproduced and studied, such as, the dynamics of phantom jam emergence (Gazis and Herman, 1992), traffic oscillations (Mauch and Cassidy, 2004), the dynamics of traffic humps (Lighthill and Whitham, 1955), metastability (Kerner and Konhäuser, 1994), traffic stability under small perturbations (Bando et al., 1995), see more details in Treiber and Kesting (2013) and Schadschneider et al. (2011). From the practical perspective, recent studies aimed to propose efficient control strategies, e.g. trajectory smoothing methods (Yao et al., 2018; Chen et al., 2014; Han et al., 2017), to reduce or eliminate the emergence of traffic oscillations; hence saving fuel consumption and reducing time delay (Li et al., 2014). To understand the generation mechanism of traffic instabilities, extensive analytical stability analysis have been carried out for both microscopic and macroscopic traffic models. The stability analysis methods include the frequency domain analysis for microscopic models (Herman et al., 1959; Mason and Woods, 1997; Ploeg et al., 2014; Monteil et al., 2019), the wave expansion technique for macroscopic models (Yi et al., 2003; Yi and Horowitz, 2006), and the indirect Lyapunov method based on eigenvalue analysis for both microscopic and macroscopic models (Bando et al., 1995; Ward, 2009; Wilson and Ward, 2011; Treiber and Kesting, 2013; Zheng et al., 2020b). The derived stability conditions mostly depend on the speed adaptation time, traffic density and drivers sensitivity to the gap and velocity difference. However, only the deterministic traffic dynamics have been considered.

In literature, various stochastic traffic models have been proposed. To our knowledge, the first developed stochastic model is the Nagel and Schreckenberg (NaSch) cellular automaton model (Nagel and Schreckenberg, 1992). It is found that the mechanism of vehicles spontaneous deceleration can reproduce the appearance of

*Corresponding authors: bjia@bjtu.edu.cn (Bin Jia), jiangrui@bjtu.edu.cn (Rui Jiang)

phantom jams. More recently, researchers have extended the cell transmission model (CTM) proposed by Daganzo (1994) to take into account uncertainties in demand and supply (SCTM) on freeways, e.g. Boel and Mihaylova (2006); Sumalee et al. (2011), CTM model with uncertainty in drivers gap choice has been studied which has the advantage of avoiding negative paths (Jabari and Liu, 2012, 2013). The fundamental diagram subject to the presence of noise has been investigated as well. For instance, LWR model with uncertainty in the free flow speed (Li et al., 2012), multiclass LWR model with uncertainty in traffic capacity as an attempt to reproduce the wide scattering in the fundamental diagram (Ngoduy, 2011), a mesoscopic model with uncertainty on transition rates and vehicles states (Qian et al., 2017), LWR model with stochastic traffic parameters including the maximum velocity, the maximum density and transitions between different traffic regimes in the velocity-density plane (Thonhofer and Jakubek, 2018). Wang and Papageorgiou (2005) used Kalman-filter to estimate traffic state by using a stochastic second-order traffic model. Read more about traffic flow dynamics with stochasticity in the book written by Chen et al. (2015). Nevertheless, the direct impact of drivers uncertainties or stochasticity on stabilizing or destabilizing traffic systems has not yet got the attention it deserves.

Recently, Jiang et al. (2014, 2018) carried out a series of experiments suggesting that speed plays an important role in stabilizing or destabilizing traffic systems. It is found that a critical speed exists below which traffic is unstable. Moreover, it was shown that the traffic instability mechanism is probabilistic and results from a competition between stochastic disturbances and speed adaptation effect.

Analytical stability analysis for stochastic traffic models still scarce in the literature and still an effervescent research issue. In this respect, recent stability analysis has been performed by using microscopic models (Treiber et al., 2006; Treiber and Kesting, 2017; Laval et al., 2014; Ngoduy et al., 2019; Xu and Laval, 2020; Wang et al., 2020; Yuan et al., 2019; Bouadi et al., 2021). It was found that stochasticity can indeed destabilize traffic systems (Treiber et al., 2006; Laval et al., 2014; Ngoduy et al., 2019; Xu and Laval, 2020), and leads to the empirically observed concave growth pattern of the cars' speed standard deviation (Wang et al., 2020; Yuan et al., 2019; Tian et al., 2021). Regarding macroscopic models, Zheng et al. (2020a) have been the first to investigate the stability properties of a stochastic LWR model and a stochastic speed gradient model. As reported in the experimental studies mentioned above, the concave growth pattern of traffic oscillations has been validated. To our knowledge, Zheng et al. (2020a) were the first to validate the concave growth pattern from a macroscopic level. However, after extensive numerical simulations, only a quantitative difference has been observed for model stability. Hence, the destabilizing effect of stochasticity has not been yet captured. Moreover, an analytical treatment to understand deeply the effect of stochasticity on traffic stability has not been yet performed.

More recently, Ngoduy (2021) has analytically investigated the stability of a general class of stochastic macroscopic models where a stability condition has been derived. Nevertheless, there are two serious deficiencies in the study. (i) From the methodological perspective, Langevin method has been used in Ngoduy (2021). However, the stability condition for a stochastic differential equation of the type $dX = AXdt + RXdW$ where X is the vector including the perturbed density and velocity for macroscopic traffic models, i.e. $X = [\rho \quad v]^T$, has been proved valid only when the matrices A and R commute (Mao, 2008), which is usually not the case in stochastic macroscopic models. (ii) As a result of (i), the stochasticity can sometimes stabilize traffic flow which is in disagreement with empirical findings and also is against Proposition 1 in Ngoduy (2021). This work attempts to address the previously mentioned deficiencies.

In this paper, we carry out an analytical stability analysis for the stochastic traffic model by using the generalized Lyapunov equation. Our analytical stability analysis will enable us to predict the appearance of traffic instabilities for different traffic situations. In particular, we will show how the presence of stochasticity can destabilize traffic flow and its dependency on the other traffic flow parameters from the macroscopic level. Moreover, we will also see that our methodology resolves the deficiency in Ngoduy (2021) in deriving stability conditions for stochastic second-order macroscopic model. Numerical simulations will be carried out for a stochastic speed gradient model to validate our theoretical analysis and the empirically observed concave growth pattern of traffic oscillations. Next, to assess the capability of the stochastic macroscopic models to reproduce the observed spontaneous emergence of traffic oscillations, the stochastic speed gradient model will be calibrated and validated against the empirical study performed by Wu et al. (2019).

Our paper will be organized as follows; in the following section, we briefly review the stochastic macroscopic model. Next, we derive a stability condition for the stochastic macroscopic model. Afterward, we carry out numerical simulations for a stochastic speed gradient model. Finally, the stochastic model will be calibrated and validated against empirical data. The last section will be devoted to a conclusion.

2 The stochastic second-order macroscopic model

Empirical observations are always revealing that real traffic flow is characterized by a certain degree of uncertainty in time and space due the stochastic nature of human drivers. After conducting a series of experiments,

Jiang et al. (2018) have demonstrated that the generation mechanism of traffic instability has a probabilistic nature. Moreover, it has been found that the presence of stochastic factors has a destabilizing effect and the generation mechanism of traffic instabilities result from a competition between the speed adaptation effect and the stochastic factors. Consequently, the existing second-order macroscopic models still can be improved by considering explicitly the presence of stochastic factors.

2.1 The stochastic model

The general stochastic second-order stochastic model reads (Ngoduy, 2021):

$$\frac{\partial \rho}{\partial t} + \frac{\partial(\rho v)}{\partial x} = g(x, t), \quad (1)$$

$$\frac{\partial v}{\partial t} + v \frac{\partial v}{\partial x} = f_1(\rho, v, \frac{\partial \rho}{\partial x}, \frac{\partial v}{\partial x}, \rho_a, v_a) + f_2(\rho, v), \quad (2)$$

Equations (1) and (2) are respectively the density and velocity equation. $g(x, t)$ is a source term which will be considered equal to zero when carrying the stability analysis (conservation of the number of vehicles). f_1 is the deterministic component of equation (2), and f_2 is the stochastic term of the form $f_2(\rho, v)dt = h(\rho, v)dW$ where h is a regular function and dW denotes the Brownian motion. In the velocity equation, the deterministic part of the right hand side encompasses the interaction term and a relaxation term reflecting the vehicles' tendency to reach a desired speed. The terms $\rho_a = \rho(x + d, t)$ and $v_a = v(x + d, t)$ are respectively the density and velocity evaluated at a distance $x + d$. Those terms account for the interaction distance in the non-local Gas Kinetic Traffic (GKT) model (Treiber et al., 1999). Due to the uncertain nature of human drivers and the estimation errors, the velocity equation (2) has been generalized by considering the presence of stochastic factors.

2.2 Existence and uniqueness of the solution

Since we are dealing with a stochastic partial differential equation, it would be interesting to check the condition of existence and uniqueness of the solution. To this aim, we apply the definition of existence and uniqueness on the stochastic continuum macroscopic model in equations (1) and (2), See Appendix A. It can be easily shown that, for regular functions f_1 and f_2 , the solution exists and unique, if (i) $\|f_2\| \leq \sigma\|x\|$, (ii) $\sigma \leq C$, where $\|\cdot\|$ is the Euclidian norm, $x = (\rho, v)$, σ is a constant and C denotes the upper bound of the Euclidian Norm of the deterministic component of equations (1) and (2).

2.3 Linearization

To carry out the stability analysis, we consider a circular road where the density of vehicles is conserved. In this study, we study the traffic stability with respect to a small deviation around the equilibrium. We linearize the above defined density and velocity equations around the equilibrium density ρ_e and velocity v_e ; hence, equations (1) and (2) become:

$$\frac{\partial \tilde{\rho}}{\partial t} + \rho_e \frac{\partial \tilde{v}}{\partial x} + v_e \frac{\partial \tilde{\rho}}{\partial x} = 0, \quad (3)$$

$$\frac{\partial \tilde{v}}{\partial t} + v_e \frac{\partial \tilde{v}}{\partial x} = \tilde{v} \frac{\partial f_1}{\partial v} + \tilde{\rho} \frac{\partial f_1}{\partial \rho} + \frac{\partial \tilde{v}}{\partial x} \frac{\partial f_1}{\partial d_v} + \frac{\partial \tilde{\rho}}{\partial x} \frac{\partial f_1}{\partial d_r} + \tilde{v}_a \frac{\partial f_1}{\partial v_a} + \tilde{\rho}_a \frac{\partial f_1}{\partial \rho_a} + (\mu \tilde{\rho} + \eta \tilde{v}) \xi(t), \quad (4)$$

where

$$\rho = \rho_e + \tilde{\rho}, \quad (5)$$

$$v = v_e + \tilde{v}, \quad (6)$$

and $d_v = \frac{\partial v}{\partial x}$, $d_r = \frac{\partial \rho}{\partial x}$. For conciseness, the following notations will also be adopted $f_{1v} = \frac{\partial f_1}{\partial v}$, $f_{1\rho} = \frac{\partial f_1}{\partial \rho}$, $f_{1v_a} = \frac{\partial f_1}{\partial v_a}$, $f_{1\rho_a} = \frac{\partial f_1}{\partial \rho_a}$, $\mu = \frac{\partial f_2}{\partial \rho}$ and $\eta = \frac{\partial f_2}{\partial v}$.

Supposing that the perturbations are given by wave equations, we consider the following Ansatz $\tilde{\rho} = \hat{\rho}(t, \omega)e^{-ikx}$ and $\tilde{v} = \hat{v}(t, \omega)e^{-ikx}$, where ω is a random event. Note that in this case, we have $\tilde{\rho}_a = \hat{\rho}e^{-ikd}$ and $\tilde{v}_a = \hat{v}e^{-ikd}$.

To simplify the analysis, we perform a first order Taylor approximation (long wave length approximation) to the previous interaction terms, i.e. $\tilde{\rho}_a = \tilde{\rho}(1 - ikd)$ and $\tilde{v}_a = \tilde{v}(1 - ikd)$. Hence, we obtain the following stochastic differential equation:

$$dx = Axdt + RxdW, \quad (7)$$

where

$$x = [\tilde{\rho} \quad \tilde{v}]^T, \quad (8)$$

and

$$A = \begin{bmatrix} ikv_e & ik\rho_e \\ f_{1\rho} + f_{1\rho a} - ikf_{1\rho x} - ikdf_{1\rho a} & f_{1v} + f_{1va} + ikv_e - ikf_{1vx} - ikdf_{1va} \end{bmatrix}, \quad (9)$$

$$R = \begin{bmatrix} 0 & 0 \\ \mu & \eta \end{bmatrix}. \quad (10)$$

The equation (7) is an autonomous stochastic differential equation for which we will derive a stability condition in the following section. To analytically derive the stability condition, we suppose that f_2 depends only on velocity (Ngoduy, 2011; Xu and Laval, 2019); hence $\mu = 0$. However, as it will be shown in Remark 4 in the following section, the Lyapunov formalism can be extended to the situation where f_2 depends on the density. In this case, numerical calculations will be needed to prove the stability condition.

3 Traffic flow stability analysis

In this section, we will derive a stability condition for equation (7) in the mean square sense. For this purpose, we first recall some important results in the theory of stochastic differential equations.

3.1 Mean square stability of stochastic differential equations

The mean square stability plays an important role in control theory. In the context of stochastic differential equations, the second moment of the solution $x(t)$ in equation (7) will tend to zero. In this work, we will use the following definition of the asymptotic mean square stability.

Definition 1 A stochastic system of the form (7) is said to be asymptotically mean square stable if:

$$\lim_{t \rightarrow \infty} E\|x(t)\|^2 = 0,$$

For any initial state $x(0) \in \mathfrak{R}^n$.

The Lyapunov formalism represents a powerful tool to prove the asymptotic stability of a given stochastic differential equation without knowing the corresponding explicit solution. In the following, we will study the mean square stability of equation (7) which has a complex valued matrix A.

Theorem 1 Consider a quadratic Lyapunov function $V(x) = x^T Px$, the autonomous stochastic differential equation (7) is mean square stable if we define a positive function $V(x)$ such that $LV(x) < 0$ (Zhang et al., 2017)

In this case, the matrix P is positive definite and $LV(x)$ is given by:

$$LV(x) = x^T (PA + A^T P + R^T P R)x. \quad (11)$$

The equation (11) is related to the differential $dV(x, t)$ by the following relation (Ito formula):

$$dV(x, t) = LV(x)dt + V_x(x)h(x)dW, \quad (12)$$

where $V_x(x)$ denotes derivative of $V(x)$ with respect to x . $h(x)$ is the stochastic component of equation (7). The above theorem only deals with real stochastic system while equation (7) is a complex valued stochastic system. In the following, we will present a method that yields the equivalent real system.

3.2 Stability analysis for the general stochastic macroscopic model

In this subsection, we exploit the previously discussed definition of the asymptotic mean square stability to extract a stability condition for equation (7) with $\mu = 0$. Hence, an approximated stability condition for the general stochastic second-order macroscopic model (equations (1) and (2)) is given by the following theorem:

Theorem 2 *The linearized stochastic differential equation given by equation (7) is mean square stable if*

$$2\rho_e - \frac{(\eta^2 + 2f_{1v} + 2f_{1va})(f_{1\rho}f_{1vx} - f_{1\rho x}f_{1v} + f_{1\rho a}f_{1vx} - f_{1\rho x}f_{1va} + d(f_{1\rho}f_{1va} - f_{1\rho a}f_{1v}))}{(f_{1\rho} + f_{1\rho a})^2} \leq 0. \quad (13)$$

Proof 1 *The linearized form of equations (1) and (2) is given by the linear stochastic differential equation (7) which has a complex valued matrix A . To apply the Lyapunov formalism, we first opt by separating the real and imaginary part of the system (7), that is, $x_s = x_r + ix_i$, where the vectors x_r and x_i are respectively the real part and imaginary part of the solution x in the system (7). Hence, the system (7) is equivalent to the following system (Zhang and Xie, 2009):*

$$dx_s = A_s x_s dt + R_s x_s dW, \quad (14)$$

where

$$x_s = [x_r \quad x_i]^T, \quad (15)$$

and

$$A_s = \begin{bmatrix} 0 & 0 & -kv_e & -k\rho_e \\ f_{1\rho} + f_{1\rho a} & f_{1v} + f_{1va} & k(f_{1\rho x} + df_{1\rho a}) & k(f_{1vx} + df_{1va} - v_e) \\ kv_e & k\rho_e & 0 & 0 \\ -k(f_{1\rho x} + df_{1\rho a}) & k(v_e - f_{1vx} - df_{1va}) & f_{1\rho} + f_{1\rho a} & f_{1v} + f_{1va} \end{bmatrix}, \quad (16)$$

$$R_s = \begin{bmatrix} 0 & 0 & 0 & 0 \\ 0 & \eta & 0 & 0 \\ 0 & 0 & 0 & 0 \\ 0 & 0 & 0 & \eta \end{bmatrix}, \quad (17)$$

Then, we consider the following quadratic Lyapunov function $V(x_s)$ which must be a positive function:

$$V(x_s) = x_s^T P x_s, \quad (18)$$

Consequently, for the stochastic system (7), the operator $LV(x)$ in equation (11) will be given by:

$$LV(x_s) = x_s^T (PA_s + A_s^T P + R_s^T P R_s) x_s. \quad (19)$$

The stochastic system (7) is stable if the operator $LV(x_s)$ has negative eigenvalues:

$$PA_s + A_s^T P + R_s^T P R_s \leq 0. \quad (20)$$

Next, we should define a positive definite matrix P such that equation (20) is negative definite and the resulting stability condition is independent of the wave number k . To perform this task, we consider a matrix P with unknown coefficients in the following equation:

$$T = PA_s + A_s^T P. \quad (21)$$

then, after simple eliminations and replacements to have a diagonal matrix T , we get the following matrix P :

$$P = \begin{bmatrix} P_1 & P_2 \\ P_2^T & P_1 \end{bmatrix}, \quad (22)$$

where the symmetric matrix P_1 reads:

$$P_1 = \begin{bmatrix} -\frac{(f_{1v} + f_{1va})(f_{1\rho}^2 + f_{1\rho a}^2 + d^2 f_{1\rho a}^2 k^2 + k^2 f_{1\rho x}^2 + 2df_{1\rho a} f_{1\rho x} k^2)}{\rho_e k^2 (f_{1\rho a} + f_{1\rho})^2} & -\frac{f_{1\rho x} + df_{1\rho a}}{f_{1\rho} + f_{1\rho a}} \\ -\frac{f_{1\rho x} + df_{1\rho a}}{f_{1\rho} + f_{1\rho a}} & -\frac{(f_{1\rho} f_{1vx} - f_{1\rho x} f_{1v} + f_{1\rho a} f_{1vx} - f_{1\rho x} f_{1va} + d(f_{1\rho} f_{1va} - f_{1\rho a} f_{1v}))}{(f_{1\rho} + f_{1\rho a})^2} \end{bmatrix}, \quad (23)$$

and the skew-symmetric matrix P_2 is given by the following:

$$P_2 = \begin{bmatrix} 0 & -\frac{1}{k} \\ \frac{1}{k} & 0 \end{bmatrix}, \quad (24)$$

After replacing in equation (19), we get the following expression:

$$LV(x) = (2\rho_e - \frac{(\eta^2 + 2f_{1v} + 2f_{1va})(f_{1\rho}f_{1vx} - f_{1\rho x}f_{1v} + f_{1\rho a}f_{1vx} - f_{1\rho x}f_{1va} + d(f_{1\rho}f_{1va} - f_{1\rho a}f_{1v}))}{(f_{1\rho} + f_{1\rho a})^2})(\tilde{v}_r^2 + \tilde{v}_i^2), \quad (25)$$

where \tilde{v}_r and \tilde{v}_i are respectively the real and imaginary components of \tilde{v} in equation (15).

The matrix P is positive definite if the following condition is met:

$$-4k^2\rho_e q_1 q_2 > 0. \quad (26)$$

$$q_1 = d^2 f_{1\rho a}^2 k^2 + 2df_{1\rho a} f_{1\rho x} k^2 + f_{1\rho}^2 + f_{1\rho a}^2 + 2f_{1\rho} f_{1\rho a} + f_{1\rho x}^2 k^2 \quad (27)$$

$$q_2 = \rho_e - \frac{(f_{1v} + f_{1va})(f_{1\rho}f_{1vx} - f_{1\rho x}f_{1v} + f_{1\rho a}f_{1vx} - f_{1\rho x}f_{1va} + d(f_{1\rho}f_{1va} - f_{1\rho a}f_{1v}))}{(f_{1\rho} + f_{1\rho a})^2} \quad (28)$$

The negativity of equation (13) implies the positivity of equation (26) with $\eta = 0$.

On the other hand, the negativity of equation (25) implies the stability condition in equation (13).

In the following, we draw some important remarks from the previously established stability condition.

Remark 1 In the deterministic case $\eta = 0$, we recover the stability condition for deterministic dynamics (Treiber and Kesting, 2013):

$$2\rho_e - \frac{(2f_{1v} + 2f_{1va})(f_{1\rho}f_{1vx} - f_{1\rho x}f_{1v} + f_{1\rho a}f_{1vx} - f_{1\rho x}f_{1va} + d(f_{1\rho}f_{1va} - f_{1\rho a}f_{1v}))}{(f_{1\rho} + f_{1\rho a})^2} \leq 0. \quad (29)$$

Remark 2 Note that in real traffic, we have the following conditions $f_{1vx} > 0$, $f_{1\rho x} < 0$, $f_{1v} < 0$, $f_{1\rho} < 0$, $f_{1va} > 0$ and $f_{1\rho a} < 0$. Hence, the term multiplied with the noise's strength η in equation (13) is always positive. Consequently, the stability condition (13) suggests that the stochastic nature of human of drivers tends to destabilize the traffic flow system.

Remark 3 For deterministic macroscopic traffic models, the stability condition in equation (29) has been obtained by eigenvalue analysis (indirect Lyapunov method). The present method is simpler and represents a fast way to obtain stability conditions for linearized macroscopic models.

Remark 4 The above stability analysis can be extended to a more general function $f_2(\rho, v)$ where ($\mu \neq 0$). However, by following the same steps in the proof, one might get a large matrix P for which positivity would be difficult to demonstrate analytically. In this case, numerical calculations are necessary to demonstrate positivity for a given parameter set.

In the following section, we will carry out numerical simulations for the stochastic speed gradient model to validate the destabilizing effect of stochasticity.

4 Numerical analysis of the stochastic speed gradient model

Due to its simplicity and capability to avoid both the wrong travel and the characteristic speed problems (Daganzo, 1995; Aw and Rascle, 2000), we will adopt the stochastic speed gradient model which is given by the following velocity equation (Jiang et al., 2002):

$$\frac{\partial v}{\partial t} + v \frac{\partial v}{\partial x} = \frac{v_e(\rho) - v}{\tau} + c_0 \frac{\partial v}{\partial x} + f_2(v), \quad (30)$$

where c_0 is the propagation speed of small disturbances, τ is the relaxation time and v_e is the equilibrium velocity.

To carry out numerical simulations, we consider a road with periodic boundary conditions. The number of cells is 500 cells where each cell has a width $\Delta x = 10$ m. The time step is $\Delta t = 0.05$ s. For simplicity, we consider the following triangular equilibrium velocity-density relationship:

$$v_e = \begin{cases} v_{max} & \rho \leq \rho_c \\ w_s \frac{\rho_{max} - \rho}{\rho} & \rho > \rho_c, \end{cases} \quad (31)$$

where the maximum velocity $v_{max} = 30$ m/s, the critical density $\rho_c = 0.02$ veh/m, the maximum density $\rho_{max} = 0.15$ veh/m and the wave speed $w_s = \frac{v_{max}\rho_c}{\rho_{max}-\rho_c} \approx 4.6$ m/s.

Regarding the stochastic term, authors have proposed different expressions of the function f_2 . For instance, Xu and Laval (2019) postulated that the Gaussian standard deviation decreases when the velocity of a vehicle tends to the maximum velocity. Ngoduy (2011) suggested that the standard deviation increases when the velocity increases. In this work, we will adopt the formulation proposed by Ngoduy (2011); hence, the following formulation of the function f_2 will be adopted:

$$f_2(v) = \sigma\sqrt{v}\xi(t), \quad (32)$$

where σ is the noise's strength or dissipation term, $\xi(t)$ is the white noise which is the derivative of the Wiener process $\xi(t) = \frac{dW(t)}{dt}$.

Indeed, on the one hand, empirical results have shown that the standard deviation of vehicles increases with increasing the mean velocity (Helbing, 2001). On the other hand, as it will be shown in the following section, the equation (32) yields good calibration and validation results against the studied experiments.

To numerically study the traffic flow evolution, we will adopt the first order upwind numerical integration scheme (Jiang et al., 2002) (See Appendix B). We will first numerically validate the previously derived stability condition and show how stochasticity can deteriorate traffic flow performance. Next, we study the capability of the stochastic speed gradient model to reproduce the empirically observed concave growth pattern of traffic oscillations.

4.1 Numerical investigation of the traffic stability

To simplify our analysis, we suppose that the propagation speed of small disturbances c_0 is constant. To obtain the stability condition for the stochastic speed gradient model, the following replacements can be made in equation (13): $f_{1vx} = c_0$, $f_{1\rho x} = 0$, $f_{1\rho a} = 0$, $f_{1va} = 0$, $f_{1v} = -\frac{1}{\tau}$ and $f_{1\rho} = \frac{v'_e}{\tau}$. Thus, we have:

$$c_0(2 - \tau\eta^2) + 2\rho_e v'_e \geq 0. \quad (33)$$

where $\eta = \frac{\sigma}{2\sqrt{v_e}}$.

In the deterministic case ($\eta = 0$), the above stability condition becomes $c_0 + \rho_e v'_e \geq 0$ which is the stability condition derived by Jiang et al. (2002).

Next, we plot the stability phase diagram of both the deterministic and stochastic speed gradient models (See Figure 1(a)). One can clearly see that as we switch on the dissipation term σ^2 from 0 m/s³ to 1 m/s³, the stability boundary shifts upward and the unstable region increases. Figure 1(a) also shows that the numerical stability boundary is in rough agreement with the theoretical one. Note that when the density is high, the analytical boundary tends to be more convex than the numerical counterpart. This difference is probably due to the effect of non-linearity which becomes more pronounced when the traffic is dense.

On the other hand, equation (33) shows that the impact of noise is proportional to relaxation time τ . Figure 1(b) displays a comparison between different relaxation time values. As the relaxation time increases, the impact of noise in destabilizing traffic performance becomes more pronounced. In other words, the impact of stochasticity becomes more severe when the agility of drivers decreases.

To give a visual representation of the impact of stochasticity on traffic flow evolution, we plot in Figure 2 the density profile for a high density value of $\rho = 0.06$ veh/m and two noise's strength values $\sigma^2 = 0$ m/s³ and $\sigma^2 = 1$ m/s³. Figure 2(a,b) show how the propagation speed of small disturbances c_0 influences the traffic stability for the deterministic case. For $c_0 = 12$ m/s, the traffic is stable while the traffic is unstable for $c_0 = 10$ m/s as predicted in Figure 1(a). On the other hand, Figure 2(c) shows how the presence of stochasticity can deteriorate traffic flow performance for $c_0 = 12$ m/s to which corresponds a stable traffic in the deterministic case. Indeed, for $\sigma^2 = 1$ m/s³, one can distinguish the emergence of traffic oscillations that are triggered by the effect of stochasticity. Finally, we show in Figure 2(d), the traffic flow evolution for the same density and dissipation coefficient but with a higher propagation speed of small disturbances. At a high value of $c_0 = 16$ m/s, traffic is stable as predicted in Figure 1(a) and only fluctuations around the equilibrium can be observed.

Finally, we compare the stability condition derived in equation (33) with the one derived by Ngoduy (2021) which is given by (after replacing in equation (24) in the paper of Ngoduy (2021)):

$$c_0(2 + \tau\eta^2) + 2\rho_e v'_e \geq 0. \quad (34)$$

From Figure 1(a), one can see that the stability condition in equation (34) predicts that stochasticity stabilizes traffic system which is neither conform with simulations nor with empirical findings. We argue that the methodology followed by Ngoduy (2021) is not suitable for studying the stability of equations (1) and (2). Indeed,

according to definition 2 in the work of Ngoduy (2021), the equation (7) is said to be almost surely linearly stochastically stable if $\Re(A - 0.5R^2) \leq 0$. However, as has been rigorously demonstrated in, e.g. Mao (2008); Gardiner (2009), the previous assertion only holds when the matrices A and R commute which is not the case in equation (7). Hence, the methodology followed by Ngoduy (2021) should be abandoned when dealing with stochastic second-order macroscopic continuum model.

4.2 The growth pattern of traffic oscillations

Recently, extensive experimental studies have been carried out to investigate the development of traffic oscillations (Jiang et al., 2018, 2014, 2015). The evolution of the standard deviation of the vehicles speed represents an efficient tool to quantify the propagation of traffic disturbances. In this respect, it was shown empirically that the growth pattern of standard deviation along the cars is concave which contradicts the prediction of deterministic traffic models. Indeed, deterministic traffic models exhibit a convex growth pattern. To address this issue, stochastic traffic flow models have been studied. It was demonstrated that stochastic traffic models can indeed reproduce the concave growth pattern, e.g. 2D-IDM model which is a stochastic version of IDM model (Jiang et al., 2014).

To verify whether the proposed stochastic macroscopic model can reproduce the concave growth pattern of traffic oscillations, we plot the evolution of the standard deviation with respect to the number of cells by increasing the value of the dissipation term σ . To carry out this task, we will consider a disturbance region where a on ramp is located. The extension of the on-ramp is supposed to be equal to 200 m. The on-ramp is located in the cell interval [480,500]. Hence, the source term of the density equation (1) will be switched on. We suppose that the on-ramp inflow is constant and equal to $q_{in} = 0.3$ veh/s. The on-ramp length will be supposed equal to $L_{rmp} = 200$ m hence $g(x, t) = \frac{q_{in}}{L_{rmp}} = 0.0015$ veh.m⁻¹/s.

In another context, Jiang and Wu (2003) showed that c_0 depends on density and has similar form to the propagation speed of small disturbances corresponding to LWR model. Accordingly, c_0 increases with density until a given density threshold (which corresponds to the critical density in LWR model), before it decreases. For simplicity, we assume that c_0 takes the following form:

$$c_0 = \begin{cases} k_1 \rho^\alpha & \rho \leq \rho_c \\ k_2 \rho^\beta & \rho > \rho_c, \end{cases} \quad (35)$$

where $\alpha > 0$ and $\beta < 0$. For simulation purpose, we assume $\alpha = 1$, $\beta = -1.2$, $k_1 = 0.35$ m ^{$\alpha+1$} /veh ^{α} · s and $k_2 = 1913$ m ^{$\beta+1$} /veh ^{β} · s. The value of ρ_c is set as $\rho_c = 0.02$ veh/m.

To perform a proper comparison, we have plotted in Figure 3, the growth pattern corresponding to different values of the dissipation term σ and the density value, $\rho = 0.03$ veh/m. As shown in Figure 3, the profile showcases a convex growth pattern of the standard deviation in the deterministic case which is not in agreement with empirical results. However, in the stochastic case, as the dissipation term σ increases, the growth pattern gradually changes from convex to concave as found in empirical investigations. Moreover, we have plotted in Figure 4 the space time diagrams of the disturbances evolution corresponding to both the deterministic and the stochastic cases. The impact of stochasticity can be seen through the stop and go waves profile in Figure 4(b). The previously mentioned results are in agreement with the last findings of Zheng et al. (2020a). We have thus confirmed that the present stochastic macroscopic model can also reproduce the empirically observed concave growth pattern.

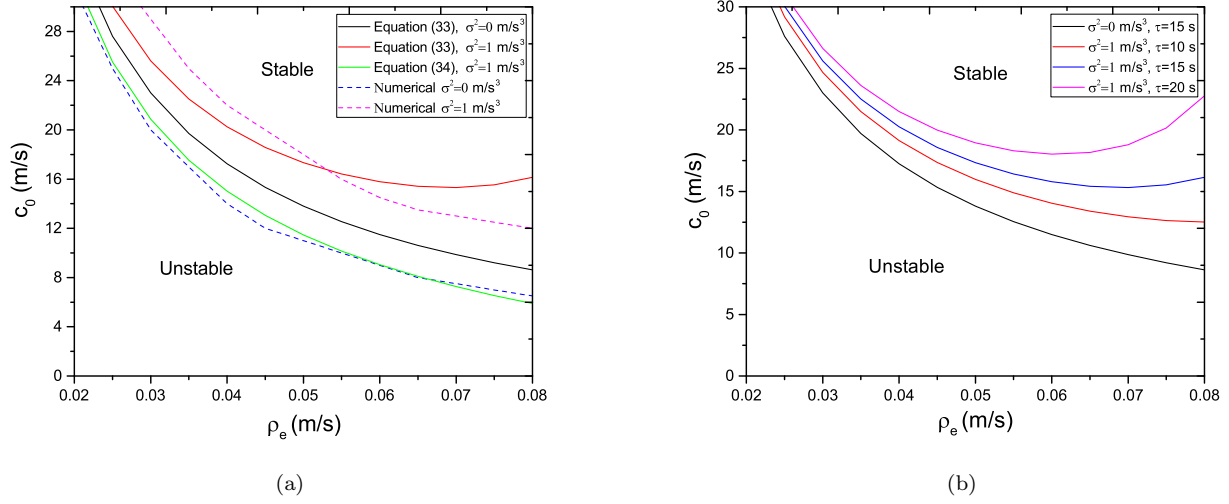


Figure 1: Stability phase diagrams of the stochastic speed gradient model in the (ρ_e, c_0) plane (a) Comparison between analytical and numerical boundaries (b) The effect of relaxation time.

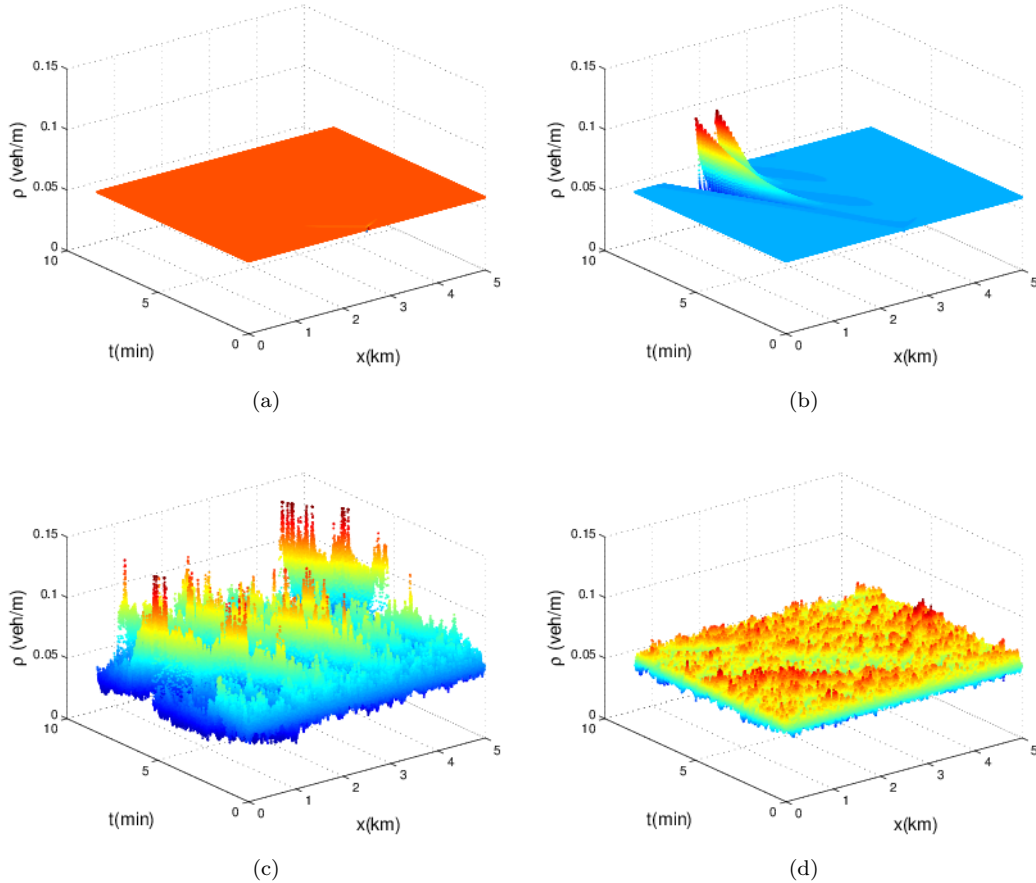


Figure 2: Traffic flow evolution for a density value $\rho = 0.06 \text{ veh/m}$ and two dissipation term values σ . (a) $c_0 = 12 \text{ m/s}$ and $\sigma^2 = 0 \text{ m/s}^3$ (b) $c_0 = 10 \text{ m/s}$ and $\sigma^2 = 0 \text{ m/s}^3$ (c) $c_0 = 12 \text{ m/s}$ and $\sigma^2 = 1 \text{ m/s}^3$ (d) $c_0 = 16 \text{ m/s}$ and $\sigma^2 = 1 \text{ m/s}^3$.

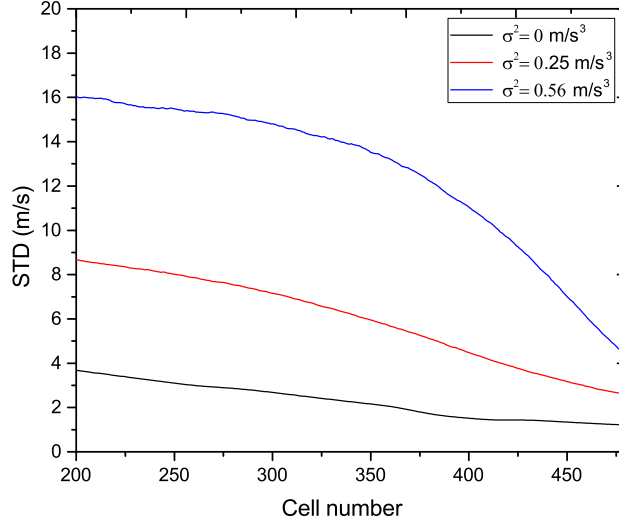


Figure 3: The growth pattern of traffic oscillations for both the deterministic and stochastic cases for the density value $\rho = 0.03$ veh/m.

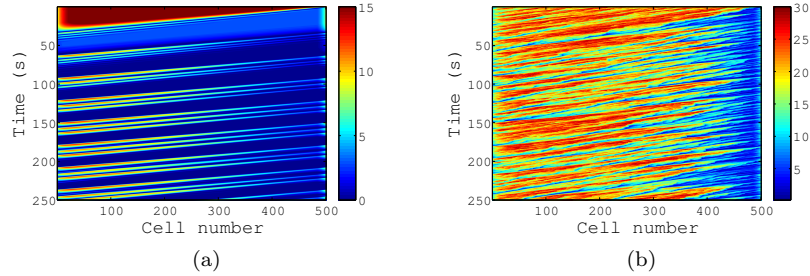


Figure 4: Space time diagrams corresponding to the density value $\rho = 0.03$ veh/m for the deterministic case and the stochastic case (a) $\sigma^2 = 0$ m/s³ (b) $\sigma^2 = 0.56$ m/s³.

5 Calibration and validation of the stochastic model

Recently, Wu et al. (2019) performed an experiment under basic conditions and low speed environment. A ring of length 260 m in circumference was considered in which the number of vehicles and thus the density varies. In those experiments, drivers were asked to follow each other as rush hour traffic. The experiments were carried out under different conditions. Since the present study deals only with a traffic situation where the presence of external perturbations is not be taken into account, the experiments A, B, C, D and E will be considered for model calibration and validation. Table 1 summarizes the details of each experiment: density, mean velocity and the standard deviation. The density is equal to the number of vehicles divided by the ring's length. In this subsection, unless stated otherwise, the density's unit will be veh/m and the velocity's unit will be m/s.

Table 1: Calibration time interval and standard deviation after space and time discretization for each experiment.

Experiment	Density (veh/m)	Calibration time interval	Standard deviation (m/s)
A	0.077	[50,400]	0.75
B	0.077	[50,400]	0.65
C	0.085	[50,350]	0.51
D	0.081	[50, 450]	0.64
E	0.073	[50,300]	0.85

Table 2: Summary of the calibration result. UW denotes the first order upwind integration scheme and MC denotes the MacCormack integration scheme

Parameter	Lower bound	Upper bound	Calibration result UW	Calibration result MC
v_{max} (m/s)	10	15	14.93	13.64
ρ_{max} (veh/m)	0.13	0.18	0.169	0.167
ρ_c (veh/m)	0.015	0.03	0.025	0.028
σ^2 (m/s ³)	0	6.25	0.47	0.16
c_0 (m/s)	4.5	10	6.01	5.65
τ (s)	1	10	6.25	7.55

Table 3: Performance index (PI) for vehicle densities used for calibration (Experiments A, C and E) and validation (Experiments B and D) by using the first order upwind integration scheme.

Density (veh/m)	PI	Standard deviation error (m/s)
0.073 (E)	0.9	0.07
0.077 (A)	0.85	0.07
0.077 (B)	0.84	0.05
0.081 (D)	0.88	0.02
0.085 (C)	0.72	0.01

In simulations, we consider the stochastic speed gradient model defined in equations (1) and (30) and a circular one dimensional road of length 260 m (as considered in the experiment). The road is subdivided into cells. The length of each cell is $\Delta x = 20$ m. Thus, the road will be composed of approximately $L = 13$ equidistant cells. A time step $\Delta t = 0.1$ s is considered. Moreover, two integration schemes will be used, the first order upwind scheme (See Appendix B) and the MacCormack method (See Appendix C). Based on the present discretization of space and time, the first integration scheme might bring about a significant amount of numerical diffusion (Treiber and Kesting, 2013; LeVeque, 1992) which may impact the quality of calibration and validation process. Due to its simplicity and its advantage of avoiding numerical diffusion (Treiber and Kesting, 2013), the MacCormack numerical integration is often preferred for simulating second order macroscopic traffic models. However, in the MacCormack method, second order numerical dispersion and oscillations near to the shock fronts are often noticed (Helbing and Treiber, 1999). It is worth mentioning that the signature of numerical diffusion is artificial smooth shocks while numerical dispersion is characterized by spurious profiles near to the shocks. Our aim is to compare between the previously mentioned numerical integration schemes in the calibration and validation process.

For both numerical integration schemes, the initial conditions for the density and the velocity are recorded from the first time step in each experiment after suppressing the transient regime in both the beginning and the end of each experiment. Next, the following performance index will be used to minimize the error between the experiments and numerical simulations for experiments A, C and E (Zheng et al., 2020a):

$$I = \sqrt{\frac{1}{LT_L} \sum_{i=1}^{i=T_L} \sum_{k=1}^{k=L} (v_{ik} - \hat{v}_{ik})^2 + (s - \hat{s})^2}, \quad (36)$$

where T_L is the maximum time step, v_{ik} is the simulated mean velocity at time step i and position k , \hat{v}_{ik} is the measured mean velocity at time step i and position k , s and \hat{s} are respectively the overall simulated and measured velocity standard deviation. The performance index is averaged over 20 initial configurations for each density. For calibration, we consider the experiments A, C and E and the fitness function in equation (36) will be averaged over all the corresponding densities. The remaining experiments, i.e. B and D will be used for validation.

Next, we use the genetic algorithm to minimize the error in equation (36). For this purpose, a population of 50 individuals has been considered. Table 1 shows for each experiment the used time interval and the overall standard deviation calculated after discretization of space and time. For both numerical integration schemes, Table 2 summarizes the used constraints for each parameter based on the results of Zheng et al. (2020a) and the calibration result for each traffic parameter: maximum velocity v_{max} , maximum density ρ_{max} , critical density ρ_c , dissipation term σ , propagation speed of small disturbances c_0 which is supposed constant and relaxation time τ . One can see that the calibration results manifest a slight difference between the first order upwind scheme and MacCormack method. Hence, the calibration result corresponding to a given integration scheme still represent a good approximation for the other in the present study where light traffic oscillations have been simulated.

To give a visual representation, we have plotted in Figure 5 and Figure 6 the simulation results of the space time diagram corresponding to each density by using the previously mentioned numerical integration schemes. Figure 5 displays the space time diagrams of experiments A, C and E which were used for calibration while Figure 6 exhibits the validation results by using experiments B and D. The performance index of each experiment

Table 4: Performance index (PI) for vehicle densities used for calibration (Experiments A, C and E) and validation (Experiments B and D) by using the MacCormack integration scheme.

Density (veh/m)	PI	Standard deviation error (m/s)
0.073 (E)	0.92	0.07
0.077 (A)	1.01	0.03
0.077 (B)	0.95	0.09
0.081 (D)	0.90	0.06
0.085 (C)	0.79	0.08

and the standard deviation error corresponding to each numerical integration scheme are reported in Table 3 and 4. Both the experimental setup and simulations display the spontaneous emergence of traffic oscillations; the presence of stochastic factors can also be distinguished.

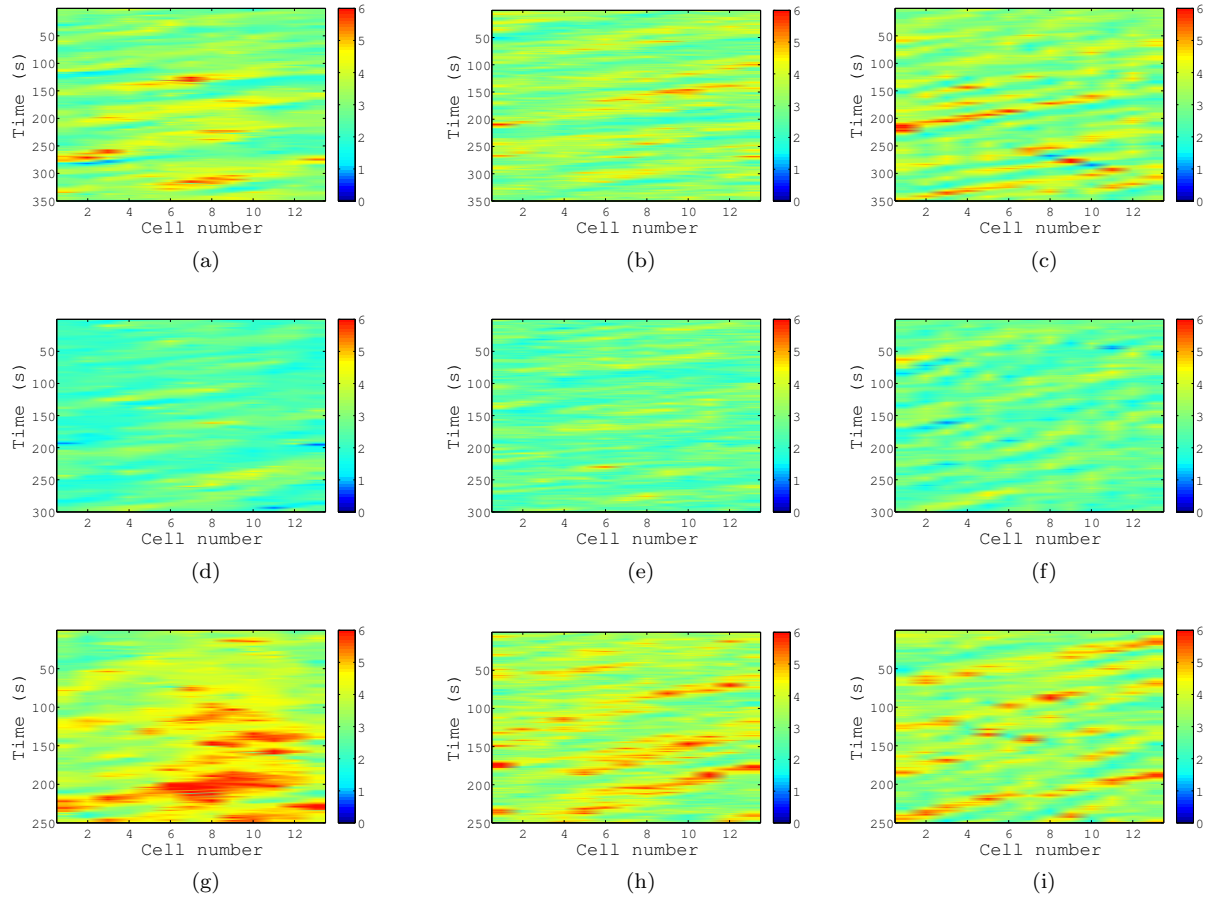


Figure 5: Space time diagrams of both the experiments (left panel), the calibrated traffic model by using the first order integration scheme (middle panel) and the calibrated traffic model by using the MacCormack integration scheme (right panel). Note that the cell number has been used in the x-axis instead of car number. (a,b,c) $\rho = 0.077$ veh/m (Experiment A) (d,e,f) $\rho = 0.085$ veh/m (Experiment C) (g,h,i) $\rho = 0.073$ veh/m (Experiment E).

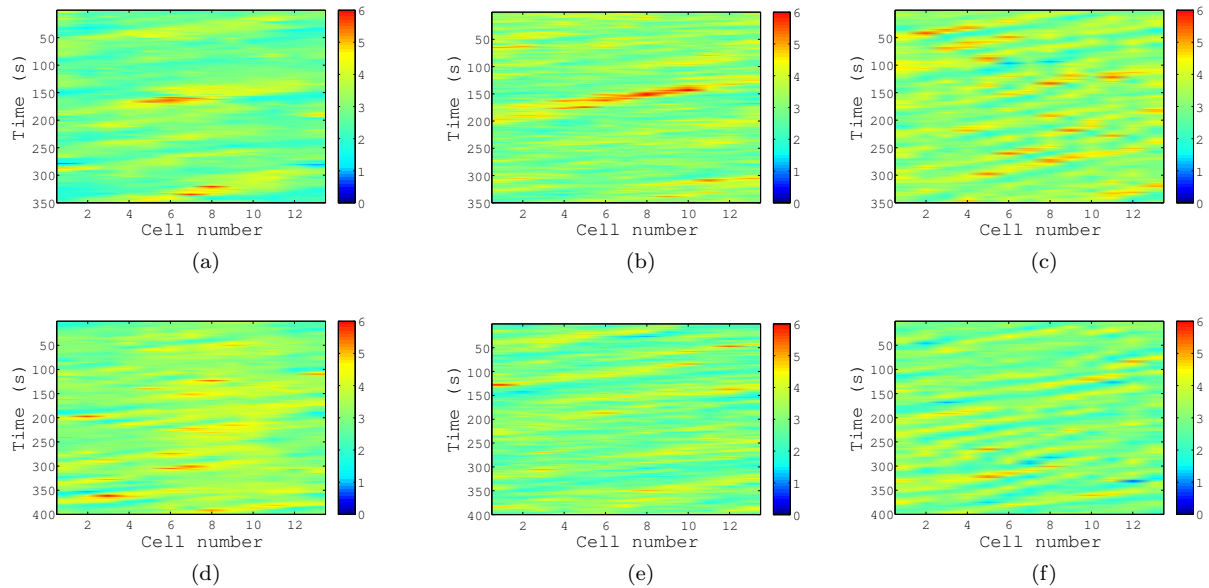


Figure 6: Space time diagrams of both the experiments (left panel), the calibrated traffic model by using the first order integration scheme (middle panel) and the calibrated traffic model by using the MacCormack integration scheme (right panel). Note that the cell number has been used in the x-axis instead of car number. (a,b,c) $\rho = 0.077$ veh/m (Experiment B) (d,e,f) $\rho = 0.081$ veh/m (Experiment D).

6 Conclusion

It is well known that the presence of noise can either stabilize or destabilize physical systems. In the vehicular traffic flow context, recent empirical investigations have demonstrated that stochastic factors play an important role in destabilizing traffic flow. In this study, we have attempted to improve the second-order macroscopic traffic models to capture the effect of stochastic factors. For the first time, a stability condition for the general stochastic second-order models has been derived by using the direct Lyapunov formalism. From the methodological perspective, we have also shown that in the traffic flow context, the direct Lyapunov method represents a simple tool to derive stability conditions for stochastic traffic models and can be extended in future works to derive stability conditions for more improved traffic models. Moreover, we have investigated the growth pattern of traffic oscillations for both deterministic and stochastic cases. In the end, the proposed stochastic model has been calibrated and validated against empirical data. Accordingly, the present research has improved the existing second-order macroscopic models in capturing the following empirical observations:

- (i) The presence of stochasticity changes qualitatively both the stochastic second-order model stability and the growth pattern of traffic oscillations.
- (ii) The stochastic second-order macroscopic traffic models can reproduce the spontaneous emergence of traffic congestion.

On the other hand, our study predicts that the impact of drivers' agility in triggering traffic instabilities increases in the presence of stochasticity. This theoretical finding still needs to be validated from empirical data.

All in all, the present study suggests that the presence of stochastic factors should be explicitly considered for a more realistic traffic flow modeling. Like stochastic microscopic models, our findings report that stochastic macroscopic models can reproduce the observed empirical features related to stochasticity. Nevertheless, further investigations should be performed for more accurate modeling of human stochastic aspects and more complex traffic situations. Finally, this work may offer a new perspective for traffic management and control by considering the stochastic nature of human drivers.

Acknowledgments

This work was supported by the National Key R & D Program of China (No. 2018YFB1600900), the National Natural Science Foundation of China (No. 71621001, 71971015 and 71931002).

References

- Aw, A. and Rascle, M. (2000). Resurrection of "second order" models of traffic flow. *SIAM Journal on Applied Mathematics*, 60:916–938.
- Bando, M., Hasebe, K., Nakayama, A., Shibata, A., and Sugiyama, Y. (1995). Dynamical model of traffic congestion and numerical simulation. *Phys. Rev. E*, 51:1035–1042.
- Boel, R. and Mihaylova, L. (2006). A compositional stochastic model for real time freeway traffic simulation. *Transportation Research Part B: Methodological*, 40:319 – 334.
- Bouadi, M., Jia, B., Jiang, R., Li, X., and Gao, Z.-Y. (2021). Traffic flow stability analysis in stochastic continuous car following models. *Submitted to Transportation Research Part B: Methodological*.
- Chen, D., Ahn, S., and Hegyi, A. (2014). Variable speed limit control for steady and oscillatory queues at fixed freeway bottlenecks. *Transportation Research Part B: Methodological*, 70:340 – 358.
- Chen, X., Li, L., and Shi, Q. (2015). *Stochastic Evolutions of Dynamic Traffic Flow: Modeling and Applications*. Springer-Verlag Berlin Heidelberg.
- Daganzo, C. F. (1994). The cell transmission model: A dynamic representation of highway traffic consistent with the hydrodynamic theory. *Transportation Research Part B: Methodological*, 28:269 – 287.
- Daganzo, C. F. (1995). Requiem for second-order fluid approximations of traffic flow. *Transportation Research Part B: Methodological*, 29:277 – 286.
- Gardiner, C. (2009). Stochastic methods: a handbook for the natural and social sciences. *Springer, Germany*.
- Gazis, D. C. and Herman, R. (1992). The moving and "phantom" bottlenecks. *Transportation Science*, 26(3):223–229.
- Han, Y., Chen, D., and Ahn, S. (2017). Variable speed limit control at fixed freeway bottlenecks using connected vehicles. *Transportation Research Part B: Methodological*, 98:113 – 134.
- Helbing, D. (2001). Traffic and related self-driven many-particle systems. *Rev. Mod. Phys.*, 73:1067–1141.
- Helbing, D. and Treiber, M. (1999). Numerical simulation of macroscopic traffic equations. *Computing in Science Engineering*, 1:89–98.
- Herman, R., Montroll, E. W., Potts, R. B., and Rothery, R. W. (1959). Traffic dynamics: Analysis of stability in car following. *Operations Research*, 7:86–106.
- Jabari, S. E. and Liu, H. X. (2012). A stochastic model of traffic flow: Theoretical foundations. *Transportation Research Part B: Methodological*, 46:156 – 174.
- Jabari, S. E. and Liu, H. X. (2013). A stochastic model of traffic flow: Gaussian approximation and estimation. *Transportation Research Part B: Methodological*, 47:15 – 41.
- Jiang, R., Hu, M.-B., Zhang, H., Gao, Z.-Y., Jia, B., and Wu, Q.-S. (2015). On some experimental features of car-following behavior and how to model them. *Transportation Research Part B: Methodological*, 80:338 – 354.
- Jiang, R., Hu, M.-B., Zhang, H. M., Gao, Z.-Y., Jia, B., Wu, Q.-S., Wang, B., and Yang, M. (2014). Traffic experiment reveals the nature of car-following. *PLOS ONE*, 9:1–9.
- Jiang, R., Jin, C.-J., Zhang, H., Huang, Y.-X., Tian, J.-F., Wang, W., Hu, M.-B., Wang, H., and Jia, B. (2018). Experimental and empirical investigations of traffic flow instability. *Transportation Research Part C: Emerging Technologies*, 94:83 – 98.
- Jiang, R. and Wu, Q.-S. (2003). Study on propagation speed of small disturbance from a car-following approach. *Transportation Research Part B: Methodological*, 37:85–99.
- Jiang, R., Wu, Q.-S., and Zhu, Z.-J. (2002). A new continuum model for traffic flow and numerical tests. *Transportation Research Part B: Methodological*, 36:405 – 419.
- Kerner, B. S. and Konhäuser, P. (1994). Structure and parameters of clusters in traffic flow. *Phys. Rev. E*, 50:54–83.

- Kloeden, P. E. and Platen, E. (1995). *Numerical solution of stochastic differential equations*. Springer-Verlag Berlin Heidelberg.
- Laval, J. A., Toth, C. S., and Zhou, Y. (2014). A parsimonious model for the formation of oscillations in car-following models. *Transportation Research Part B: Methodological*, 70:228 – 238.
- LeVeque, R. J. (1992). Numerical methods for conservation laws (2nd edition). *Birkhäuser Basel*.
- Li, J., Chen, Q.-Y., Wang, H., and Ni, D. (2012). Analysis of lwr model with fundamental diagram subject to uncertainties. *Transportmetrica*, 8:387–405.
- Li, X., Cui, J., An, S., and Parsafard, M. (2014). Stop-and-go traffic analysis: Theoretical properties, environmental impacts and oscillation mitigation. *Transportation Research Part B: Methodological*, 70:319 – 339.
- Lighthill, M. J. and Whitham, G. B. (1955). On kinematic waves. ii. a theory of traffic flow on long crowded roads. *Proceedings of the Royal Society of London. Series A, Mathematical and Physical Sciences*, 229(1178):317–345.
- MacCormack, R. W. (2002). *The Effect of Viscosity in Hypervelocity Impact Cratering, Frontiers of Computational Fluid Dynamics 2002*, pages 27–43.
- Mao, X. (2008). Stochastic differential equations and applications, horwood, second edition.
- Mason, A. D. and Woods, A. W. (1997). Car-following model of multispecies systems of road traffic. *Phys. Rev. E*, 55:2203–2214.
- Mauch, M. and Cassidy, M. J. (2004). Freeway Traffic Oscillations: Observations and Predictions. University of California Transportation Center, Working Papers qt89c3h1vv, University of California Transportation Center.
- Monteil, J., Bouroche, M., and Leith, D. J. (2019). \mathcal{L}_2 and \mathcal{L}_∞ stability analysis of heterogeneous traffic with application to parameter optimization for the control of automated vehicles. *IEEE Transactions on Control Systems Technology*, 27:934–949.
- Nagel, K. and Schreckenberg, M. (1992). A cellular automaton model for freeway traffic. *Journal de Physique I*, 2:2221–2229.
- Ngoduy, D. (2011). Multiclass first-order traffic model using stochastic fundamental diagrams. *Transportmetrica*, 7:111–125.
- Ngoduy, D. (2021). Noise-induced instability of a class of stochastic higher order continuum traffic models. *Transportation Research Part B: Methodological*, 150:260–278.
- Ngoduy, D., Lee, S., Treiber, M., Keyvan-Ekbatani, M., and Vu, H. (2019). Langevin method for a continuous stochastic car-following model and its stability conditions. *Transportation Research Part C: Emerging Technologies*, 105:599 – 610.
- Ploeg, J., van de Wouw, N., and Nijmeijer, H. (2014). Lp string stability of cascaded systems: Application to vehicle platooning. *IEEE Transactions on Control Systems Technology*, 22:786–793.
- Qian, W.-L., Siqueira, A. F., Machado, R. F., Lin, K., and Grant, T. W. (2017). Dynamical capacity drop in a nonlinear stochastic traffic model. *Transportation Research Part B: Methodological*, 105:328 – 339.
- Schadschneider, A., Chowdhury, D., and Nishinari, K. (2011). Elsevier, Amsterdam.
- Sumalee, A., Zhong, R., Pan, T., and Szeto, W. (2011). Stochastic cell transmission model (sctm): A stochastic dynamic traffic model for traffic state surveillance and assignment. *Transportation Research Part B: Methodological*, 45(3):507 – 533.
- Thonhofer, E. and Jakubek, S. (2018). Investigation of stochastic variation of parameters for a macroscopic traffic model. *Journal of Intelligent Transportation Systems*, 22:547–564.
- Tian, J., Zhu, C., Chen, D., Jiang, R., Wang, G., and Gao, Z. (2021). Car following behavioral stochasticity analysis and modeling: Perspective from wave travel time. *Transportation Research Part B: Methodological*, 143:160 – 176.

- Treiber, M., Hennecke, A., and Helbing, D. (1999). Derivation, properties, and simulation of a gas-kinetic-based, nonlocal traffic model. *Phys. Rev. E*, 59:239–253.
- Treiber, M. and Kesting, A. (2013). *Traffic Flow Dynamics, Data, Models and Simulation*. Springer-Verlag Berlin Heidelberg.
- Treiber, M. and Kesting, A. (2017). The intelligent driver model with stochasticity -new insights into traffic flow oscillations. *Transportation Research Procedia*, 23:174 – 187.
- Treiber, M., Kesting, A., and Helbing, D. (2006). Delays, inaccuracies and anticipation in microscopic traffic models. *Physica A: Statistical Mechanics and its Applications*, 360:71 – 88.
- Wang, Y., Li, X., Tian, J., and Jiang, R. (2020). Stability analysis of stochastic linear car-following models. *Transportation Science*, 54:274–297.
- Wang, Y. and Papageorgiou, M. (2005). Real-time freeway traffic state estimation based on extended kalman filter: a general approach. *Transportation Research Part B: Methodological*, 39:141 – 167.
- Ward, J. A. (2009). *Heterogeneity, Lane-Changing and Instability in Traffic: A Mathematical Approach*. Doctoral diss., University of Bristol.
- Wilson, R. and Ward, J. (2011). Car-following models: fifty years of linear stability analysis – a mathematical perspective. *Transportation Planning and Technology*, 34:3–18.
- Wu, F., Stern, R. E., Cui, S., Monache], M. L. D., Bhadani, R., Bunting, M., Churchill, M., Hamilton, N., Haulcy, R., Piccoli, B., Seibold, B., Sprinkle, J., and Work, D. B. (2019). Tracking vehicle trajectories and fuel rates in phantom traffic jams: Methodology and data. *Transportation Research Part C: Emerging Technologies*, 99:82 – 109.
- Xu, T. and Laval, J. (2020). Statistical inference for two-regime stochastic car-following models. *Transportation Research Part B: Methodological*, 134:210 – 228.
- Xu, T. and Laval, J. A. (2019). Analysis of a two-regime stochastic car-following model: Explaining capacity drop and oscillation instabilities. *Transportation Research Record*, 2673:610–619.
- Yao, H., Cui, J., Li, X., Wang, Y., and An, S. (2018). A trajectory smoothing method at signalized intersection based on individualized variable speed limits with location optimization. *Transportation Research Part D: Transport and Environment*, 62:456 – 473.
- Yi, J. and Horowitz, R. (2006). Macroscopic traffic flow propagation stability for adaptive cruise controlled vehicles. *Transportation Research Part C: Emerging Technologies*, 14:81–95.
- Yi, J., Lin, H., Alvarez, L., and Horowitz, R. (2003). Stability of macroscopic traffic flow modeling through wavefront expansion. *Transportation Research Part B: Methodological*, 37:661–679.
- Yuan, K., Laval, J., Knoop, V. L., Jiang, R., and Hoogendoorn, S. P. (2019). A geometric brownian motion car-following model: towards a better understanding of capacity drop. *Transportmetrica B: Transport Dynamics*, 7:915–927.
- Zhang, W. and Xie, L. (2009). Interval stability and stabilization of linear stochastic systems. *IEEE Transactions on Automatic Control*, 54:810–815.
- Zhang, W., Xie, L., and Chen, B.-S. (2017). *Stochastic h_2/h_∞ control: A nash game approach (1st ed.)*. Taylor and Francis.
- Zheng, S.-T., Jiang, R., Jia, B., Tian, J., and Gao, Z. (2020a). Impact of stochasticity on traffic flow dynamics in macroscopic continuum models. *Transportation Research Record*, 2674:690–704.
- Zheng, Y., Wang, J., and Li, K. (2020b). Smoothing traffic flow via control of autonomous vehicles. *IEEE Internet of Things Journal*, 7:3882–3896.

Appendix A. Existence and uniqueness of the solution

Definition 1 Consider the following stochastic differential equation:

$$dX = f(x, t)dt + h(x, t)dW. \quad (37)$$

(i) The solution of (37) exists if the following condition is satisfied (linear growth) (Zhang et al., 2017):

$$\|f(x, t)\| + \|g(x, t)\| \leq \lambda_1(1 + \|x\|). \quad (38)$$

This condition guarantees that the solution does not blow up from a given time step, i.e. the solution does not have finite time escape.

(ii) The solution of (37) is unique if the following condition is satisfied (Lipschitz continuity) (Zhang et al., 2017):

$$\|f(x, t) - f(y, t)\| + \|g(x, t) - g(y, t)\| \leq \lambda_2\|x - y\|. \quad (39)$$

λ_1 and λ_2 are positive constants and $\|\cdot\|$ denotes the Euclidean norm.

We apply the above definition to the stochastic continuum macroscopic model in equations (1) and (2) by considering $f(x, t) = (s, f_1)$, $s = -\frac{\partial \rho v}{\partial x}$, $h(x, t) = (0, f_2)$ and $x = (\rho, v)$.

(i) Existence:

The deterministic model is hyperbolic which ensures the existence of solution given an initial condition; hence, the Euclidean norm $\|f(x, t)\|$ is finite, namely, $\|f(x, t)\| \leq C$. Moreover, assume $\|h(x, t)\| \leq \sigma\|x\|$, Hence:

$$\|f(x, t)\| + \|g(x, t)\| \leq C + \sigma\|x\| = C(1 + \frac{\sigma}{C}\|x\|). \quad (40)$$

Consequently, the following inequality:

$$C(1 + \frac{\sigma}{C}\|x\|) \leq C(1 + \|x\|), \quad (41)$$

is guaranteed if $\frac{\sigma}{C} \leq 1$. The dissipation parameter σ should be smaller than the upper bound of the Euclidean norm of the function f to guarantee existence.

(ii) Uniqueness

The functions f and h are both continuous and differentiable; hence, after applying the intermediate value theorem, we get:

$$\|f(x, t) - f(y, t)\| \leq m_1\|x - y\|, \quad (42)$$

$$\|h(x, t) - h(y, t)\| \leq m_2\|x - y\|, \quad (43)$$

The summation of the above inequalities yield:

$$\|f(x, t) - f(y, t)\| + \|g(x, t) - g(y, t)\| \leq \lambda_2\|x - y\|, \quad (44)$$

where $\lambda_2 = m_1 + m_2$. Consequently, the solution is unique.

Appendix B. First order upwind scheme

In numerical simulations, we have applied the numerical integration method firstly proposed by Jiang et al. (2002) for the deterministic speed gradient model. For the stochastic component, we have adopted the Euler-Maruyama integration scheme (Kloeden and Platen, 1995).

For density equation update, the following discretization form has been used:

$$\tilde{\rho}_i^{j+1} = \rho_i^j - \frac{dt}{dx}(v_{i+1}^j - v_i^j)\rho_i^j - \frac{dt}{dx}v_i^j(\rho_i^j - \rho_{i-1}^j) + g(x, t)dt. \quad (45)$$

It has been demonstrated that the equation (45) ensures the suitable physical direction of the information propagation (Jiang et al., 2002).

For the velocity equation, the following integration scheme is adopted:

if $v_i^j < c_0$:

$$\tilde{v}_i^{j+1} = v_i^j - \frac{dt}{dx}(v_i^j - c_0)(v_{i+1}^j - v_i^j) - dt \frac{(v_i^j - v_e)}{\tau} - \sigma\sqrt{v_i^j}dB_i^j(t). \quad (46)$$

if $v_i^j \geq c_0$:

$$\tilde{v}_i^{j+1} = v_i^j - \frac{dt}{dx}(v_i^j - c_0)(v_i^j - v_{i-1}^j) - dt \frac{(v_i^j - v_e)}{\tau} + \sigma\sqrt{v_i^j}dB_i^j(t). \quad (47)$$

where $dB_i^j(t)$ is a normal distribution of mean 0 and standard deviation dt .

Appendix C. MacCormack integration scheme

In MacCormack integration scheme (MacCormack, 2002), we first approximate the solution at a given time step by a predictor in which the upwind scheme is used. In the upwind scheme, we take the information coming from the upstream traffic direction. Consequently, for the predictor, the density equation (1) reads:

$$\tilde{\rho}_i^{j+1} = \rho_i^j - \frac{dt}{dx}(\rho_i^j v_i^j - \rho_{i-1}^j v_{i-1}^j). \quad (48)$$

For the non-conservative velocity equation (30), the discretization is as the following:

$$\tilde{v}_i^{j+1} = v_i^j - \frac{dt}{dx}(v_i^j - c_0)(v_i^j - v_{i-1}^j) - dt \frac{(v_i^j - v_e)}{\tau}. \quad (49)$$

After calculating the predictor, we calculate the corrector which is the arithmetic mean between the predictor in equations (48) and (49) and the following density and velocity equations by taking into account the downwind scheme (information coming from the downstream traffic direction):

$$\hat{\rho}_i^{j+1} = \rho_i^j - \frac{dt}{dx}(\hat{\rho}_{i+1}^j \tilde{v}_{i+1}^j - \tilde{\rho}_i^j \hat{v}_i^j). \quad (50)$$

$$\hat{v}_i^{j+1} = v_i^j - \frac{dt}{dx}(\tilde{v}_i^j - c_0)(\tilde{v}_{i+1}^j - \hat{v}_i^j) - dt \frac{(\tilde{v}_i^j - v_e)}{\tau}. \quad (51)$$

Hence, the density and velocity updates are given by:

$$\rho_i^{j+1} = \frac{1}{2}(\tilde{\rho}_i^{j+1} + \hat{\rho}_i^{j+1}) \quad (52)$$

$$v_i^{j+1} = \frac{1}{2}(\tilde{v}_i^{j+1} + \hat{v}_i^{j+1}) + \sigma \sqrt{v_i^j} dB_i^j(t) \quad (53)$$